Nonclassical Pathways for Silsesquioxane Growth

Karl Jug* and Igor P. Gloriozov†

Theoretische Chemie, Universität Hannover, Am Kleinen Felde 30, 30167 Hannover, Germany

Received: December 31, 2001; In Final Form: February 28, 2002

The mechanism of silsesquioxane growth is studied with an insertion mechanism analogous to the one previously proposed for fullerene growth. Different from previous work, the possibility of the involvement of larger rings with $(SiO)_7$ size in cages of hydridosilsesquioxanes $Si_nO_{3n/2}H_n$ is investigated. Such a nonclassical pathway is calculated for the growth of $Si_{30}O_{45}H_{30}$ via $Si_{32}O_{48}H_{32}$ to $Si_{34}O_{51}H_{34}$. The MSINDO method is used to determine the transition structures and intermediates. It is found that nonclassical pathways are equally preferable as classical pathways involving cages with $(SiO)_5$ and $(SiO)_6$ rings only.

1. Introduction

The importance of siloxanes in chemical vapor deposition (CVD) processes has been repeatedly discussed.[1,2] In the combustion of $SiCl_4$ in O_2, which leads to silicon dioxide, hundreds of intermediates of chlorosiloxanes have been detected.[3−5] Such cluster compounds can be considered as connecting links between molecules and solids. Among the siloxanes, the silsesquioxanes of composition $Si_nO_{3n/2}R_n$ (R = Cl, H, or other substituents) are most interesting. They form cages which can be functionalized[6−8] and can serve as precursors of tailor-made heterogeneous catalyst centers.[9] Among the silsesquioxanes, the cube-shaped cage of $Si_8O_{12}R_8$ was most often the subject of experimental investigations. Until recently, only silsesquioxanes with up to 18 Si atoms were synthesized[10,11] and analyzed. However, the recent preparation of Rikowski and Marsmann[12] of mixtures of higher silsesquioxanes by base-catalyzed cage rearrangement of octasilsesquioxanes opened the way into new dimensions. The MALDI-TOF (Matrix-Assisted Laser Desorption/Ionization Time-Of-Flight) mass spectrometric analysis of these mixtures by Krüger et al.[13] extended the size of detected silsesquioxanes to $n = 38$. Our own interest derived from the work of Binnewies and his group and was concentrated initially on chlorosilsesquioxanes with up to 60 silicon atoms.[14] In this previous paper, we presented the binding energy per silicon atom of a variety of $Si_nO_{3n/2}Cl_n$ compounds ranging from $Si_4O_6Cl_4$ to $Si_{60}O_{90}Cl_{60}$. When we realized that the postulated structures of $Si_{24}O_{36}Cl_{24}$ as sodalite cage and $Si_{48}O_{72}Cl_{48}$ as distorted α-cage could not be the global minima, because their energies did not fit to the energy versus size curve, we repeated the calculations with the MSINDO method for hydridosilsesquioxanes[15] $Si_nO_{3n/2}H_n$ method.[16,17] This is an improved version of the SINDO1 method[18,19] which was applied to silicon compounds.[20,21] Even more essential than the improvement of structural and energetic data was the discovery that the most stable of the larger silsesquioxane compounds contained only $(SiO)_5$ and $(SiO)_6$ rings. This opened the way to use information[22] derived for fullerenes where C_5 and C_6 rings were structure-determining. However, different from our expectation, the most stable $Si_{48}O_{72}H_{48}$ and $Si_{60}O_{90}H_{60}$ cages had egg-shaped structures. We therefore extended our calculations to even larger silsesquioxanes of D_{6d} and D_{6h} symmetry up to $Si_{240}O_{360}H_{240}$,[23] which one could consider as precursors of nanotubes. To connect these structures by a growth mechanism, we postulated that an insertion[15] of the formal unit $Si_2O_3H_2$ analogous to the C_2 insertion in fullerenes could explain the growth. The interest in nanotubes is not restricted to carbon nanotubes, but tubular structures of silicon[24] and siloxenes[25] were recently predicted by density functional tight-binding studies.

SCHEME 1

SCHEME 2

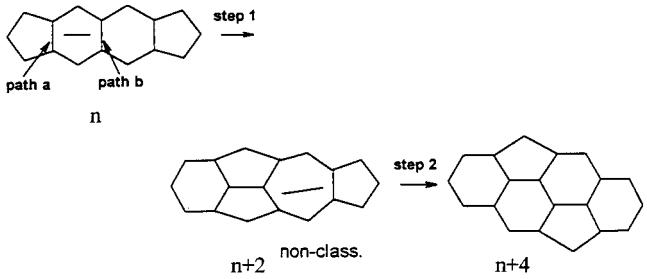

It was therefore only consequential that we investigated the growth of hydridosilsesquioxanes by the postulated insertion mechanism both qualitatively and quantitatively.[26] From a qualitative analysis, it became clear that an insertion mechanism, which tries to retain only $(SiO)_5$ and $(SiO)_6$ rings in the cages, would not be able to reach the D_{6d} or D_{6h} structures beyond $Si_{60}O_{90}H_{60}$. The quantitative analysis confirmed the feasibility of insertion at higher temperatures but predicted that isomerization would not be possible. We therefore now went farther to explore the possibility of nonclassical pathways involving $(SiO)_7$ rings in the formation of larger silsesquioxane cages via the insertion mechanism. This would open the way to the occurrence of larger nanotube structures of high symmetry. In fullerenes, such nonclassical structures have been predicted.[27−30]

2. Nonclassical Structures for Silsesquioxane Growth

In a previous paper,[26] we had pursued the insertion mechanism that we had postulated.[15] Formally, a $Si_2O_3H_2$ unit has to be inserted into a silsesquioxane cage bridging a hexagon of Si

* To whom correspondence should be addressed.
† Visiting scientist; permanent address: Department of Chemistry, Moscow State University, Moscow 119 899, Russia.

10.1021/jp014708r CCC: $22.00
Published on Web 04/17/2002

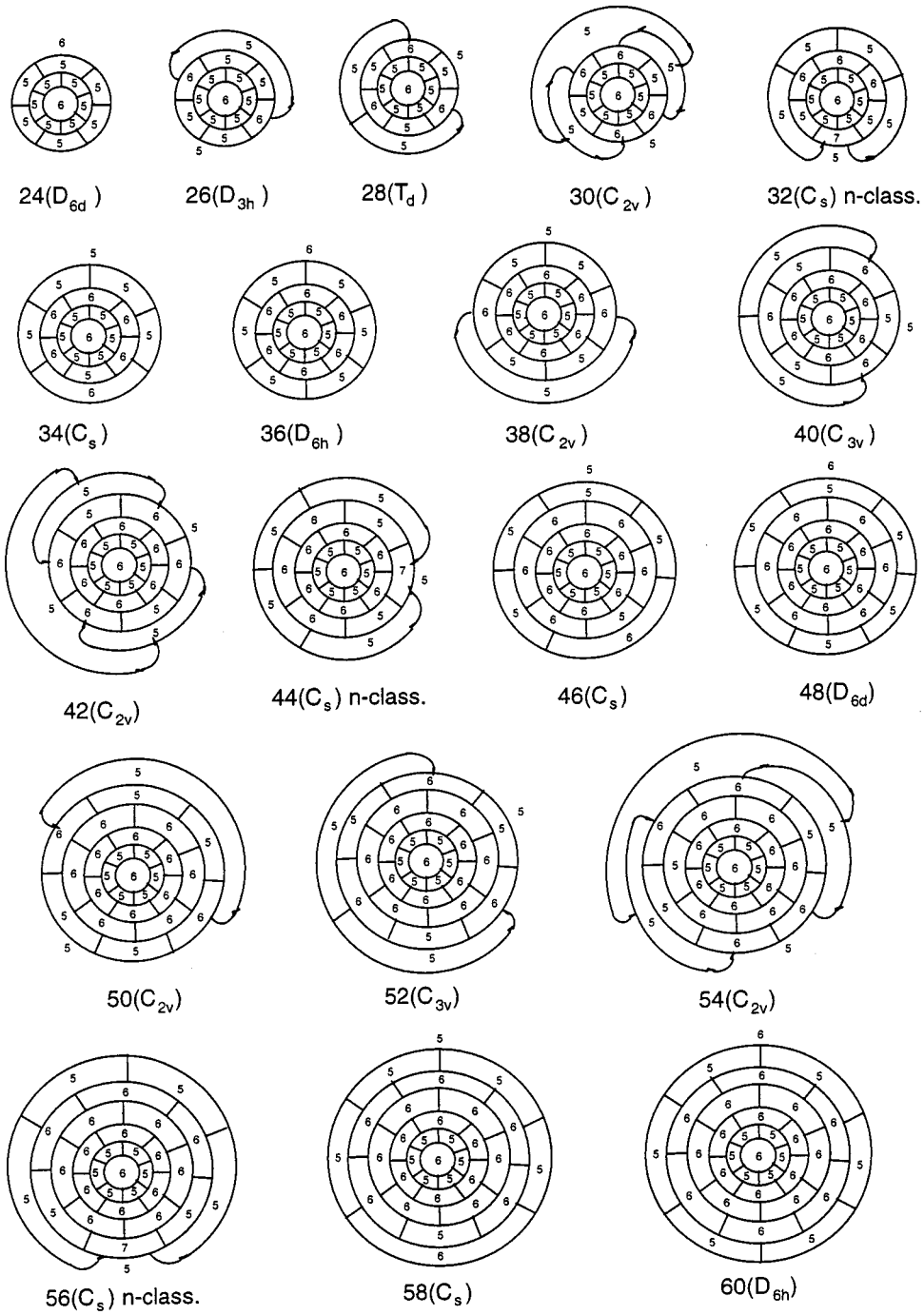

Figure 1. Schlegel diagrams for a nonclassical pathway from $Si_{24}O_{36}H_{24}$ to $Si_{60}O_{90}H_{60}$.

atoms connected by more floppy oxygen atoms. This hexagon is converted into two pentagons. In the classical pathway,[15,26] the two pentagons adjacent to the hexagon are converted into hexagons (Scheme 1). If one of the adjacent rings is a hexagon, this will be converted into a heptagon (Scheme 2), which represents a nonclassical structure in the fullerene terminology.[31] In contrast, classical fullerenes consist of pentagons and hexagons only. Silsesquioxanes have the shape of cages which usually consist of rings containing five or six silicon atoms. These Si atoms are connected by O atoms. The difference between the fullerene cages and the silsesquioxane cages is that the latter do not obey the isolated-pentagon rule. According to Fowler et al.,[31] a heptagon is perhaps the most natural departure from the fullerene recipe because it constitutes the minimal deviation from the hexagon, the most numerous ring in a large

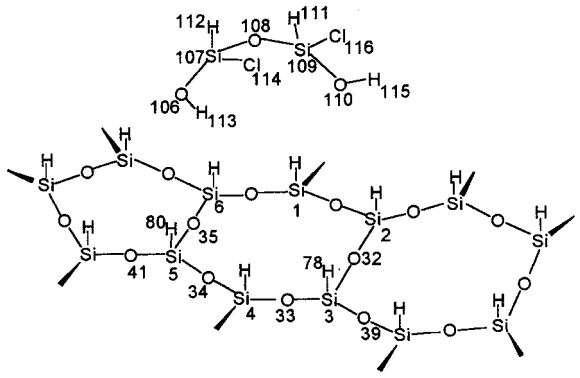

Figure 2. Approach of $(SiOHClH)_2O$ to $Si_{30}O_{45}H_{30}$ for reaction pathway a (step 1).

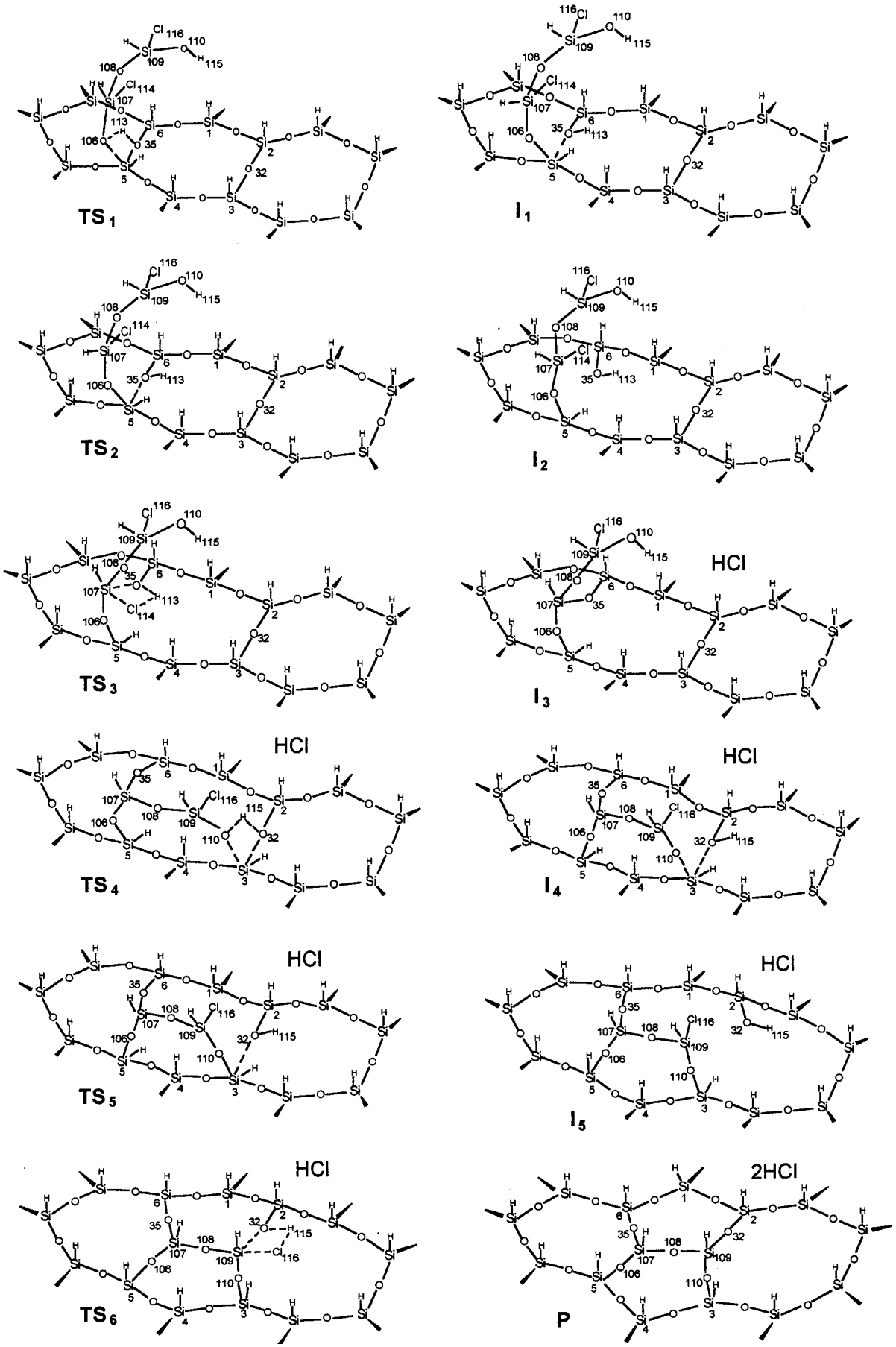

Figure 3. Transition structures TS and intermediates I for reaction pathway a (step 1) from classical structure $Si_{30}O_{45}H_{30}$ to nonclassical structure $Si_{32}O_{48}H_{32}$.

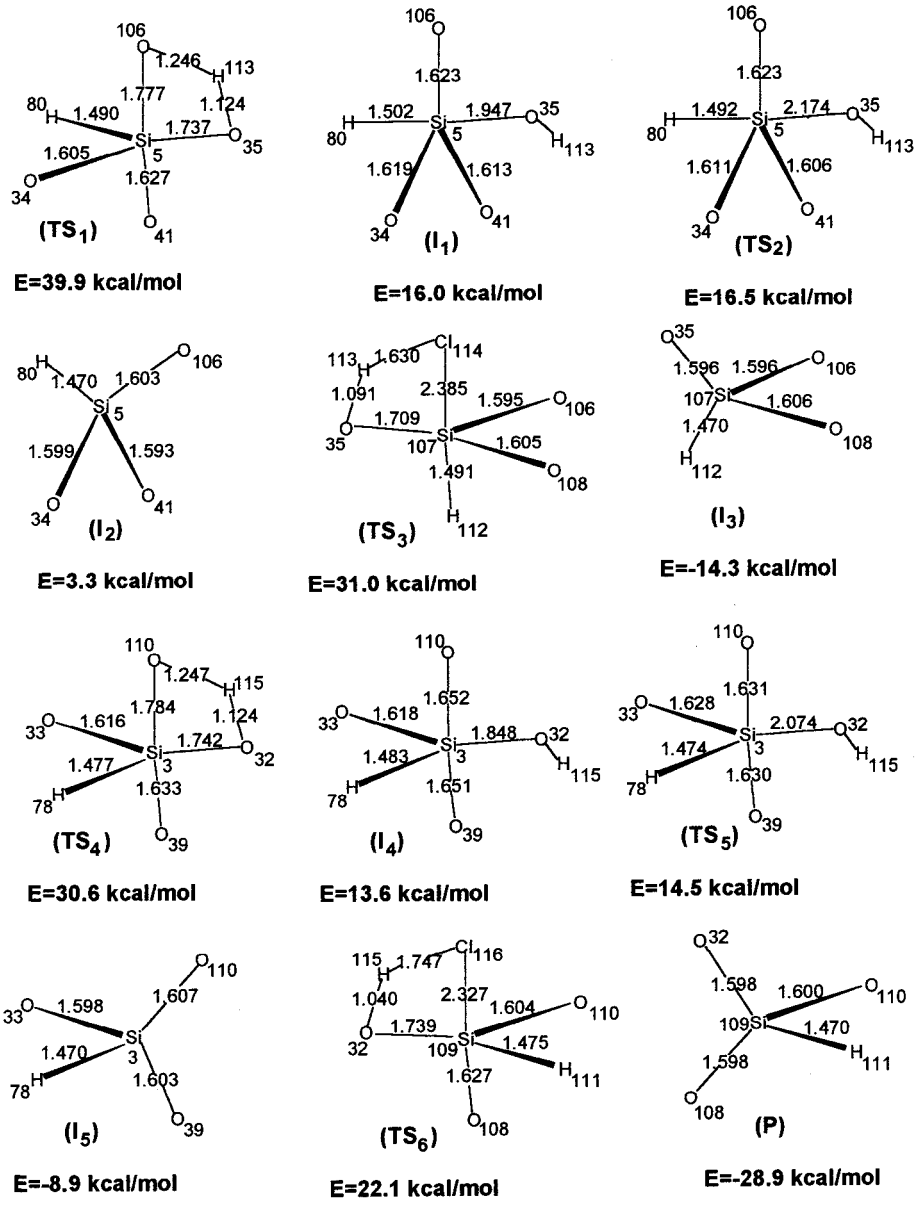

Figure 4. Energy and structure data for reaction pathway a (step 1).

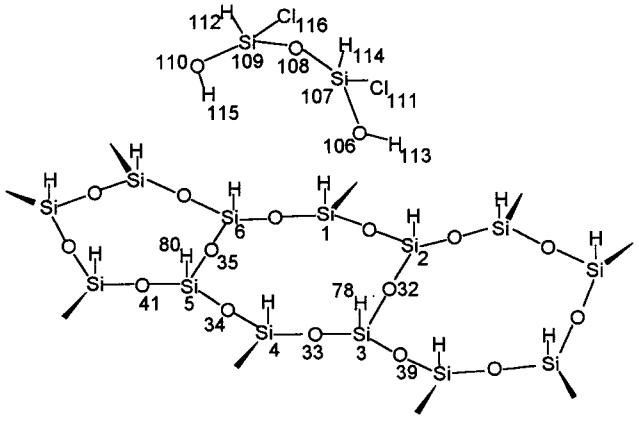

Figure 5. Approach of $(SiOHClH)_2O$ to $Si_{30}O_{45}H_{30}$ for reaction pathway b (step 1).

fullerene cage. There are two pathways a and b for step 1 of such a nonclassical process. In step 2, involving the insertion of another $Si_2O_3H_2$ unit, the heptagon can be reduced again to a hexagon, thus leading back to a classical structure. In Figure 1, we show now a series of Schlegel diagrams,[22] which illustrate how the compound $Si_{24}O_{36}H_{24}$ of D_{6d} symmetry can be converted into $Si_{60}O_{90}H_{60}$ of D_{6h} symmetry via the highly symmetric structures $Si_{36}O_{54}H_{36}$ (D_{6h}) and $Si_{48}O_{72}H_{98}$ (D_{6d}). To achieve this, three nonclassical structures with $n = 32$, 44, and 56 must be generated. This is definitely different from the classical pathways described previously.[26] In the following, we present detailed calculations for the steps from $n = 30$ to 32 and from $n = 32$ to 34.

3. Nonclassical Pathways

3.1 Conversion of $Si_{30}O_{45}H_{30}$ to $Si_{32}O_{48}H_{32}$.

Figure 2 shows the relevant portion of reactant $Si_{30}O_{45}H_{30}$ and the reagent $(SiOHClH)_2O$, which contains the $Si_2O_3H_2$ unit, in the approach of pathway a (Scheme 2). The idea is now to go through a series of steps which eventually removes two HCl molecules from the system and leads to a nonclassical structure of $Si_{32}O_{48}H_{32}$ after step 1 in Scheme 2.

The following calculations were performed with the MSINDO method[16,17] which is a highly improved modification of the SINDO1 method[18,19] for the first- and second-row elements in these reactions. This concerns both structure and stability predictions. The reason is that we parametrized small molecules

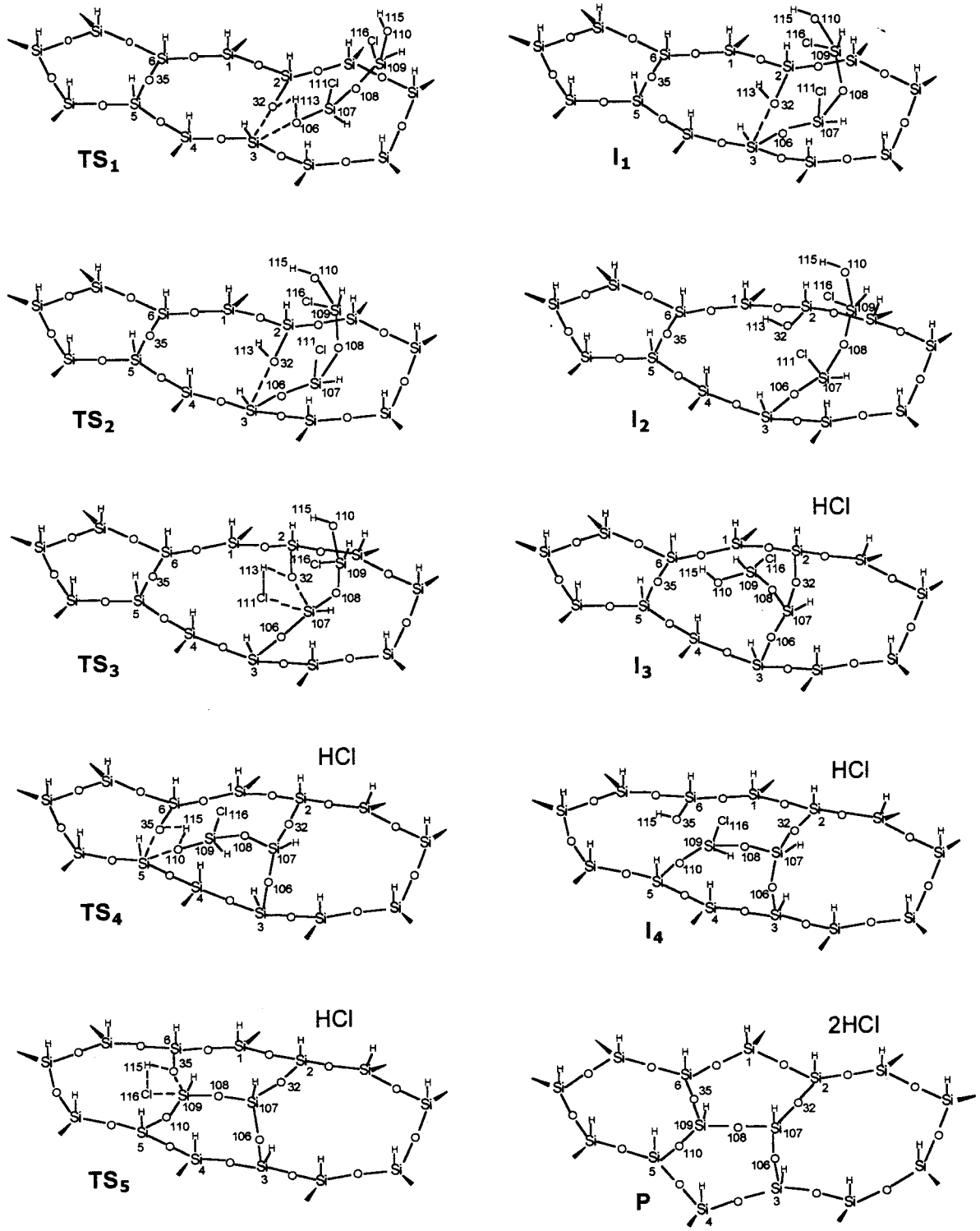

Figure 6. Transition structures TS and intermediates I for reaction pathway b (step 1) from classical structure $Si_{30}O_{45}H_{30}$ to nonclassical structure $Si_{32}O_{48}H_{32}$.

with first- and second- row elements with respect mainly to structure and heats of reaction.[15] The average accuracy is documented with respect to experimental data and compared with other semiempirical methods.[16] We have documented the high accuracy of MSINDO in siloxanes for the structures of Si_2OH_6 and $Si_8O_{12}H_8$.[15] The accuracy of our silsesquioxane structures appears to be at least equally good as in local density approximation (LDA) calculations with density functional theory (DFT) and better than the reported nonlocal density approximation (NLDA) values.[32] Further work[33] of this group was concerned with polarizabilities and hyperpolarizabilities of H-silsesquioxanes at the INDO/CI level, where the suitability of these compounds as nonlinear optical materials was tested. Figure 3 shows the reaction steps, that is, transition structures TS and intermediates I involved in pathway a. The transition structures are characterized by one negative root of the Hessian of the energy. In TS_1, one OH group of the reagent approaches an Si−O bond between the hexagon and the left pentagon and loosens it. In the following intermediate I_1, the attacking O_{106} atom binds to the Si_5 atom of the cage and H_{113} binds to the loosened O_{35}. Figure 4 shows the neighborhood of the relevant Si_5 atom in terms of the structural data. A barrier of 39.9 kcal/

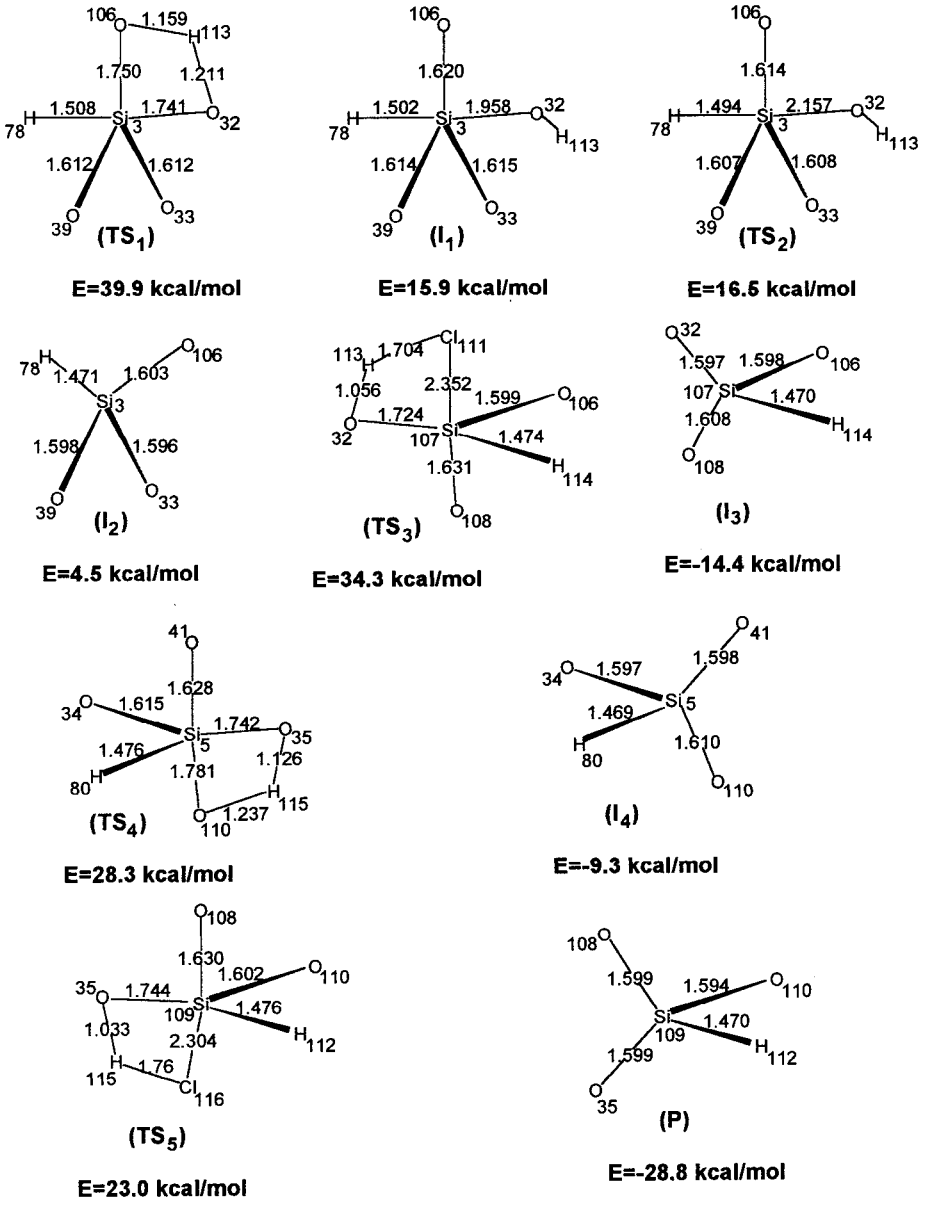

Figure 7. Energy and structure data for reaction pathway b (step 1).

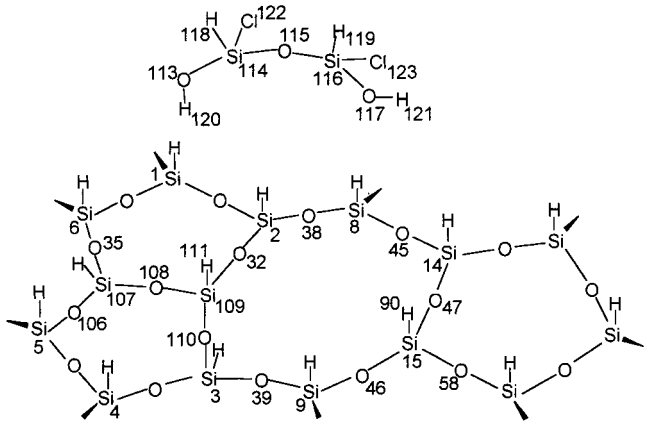

Figure 8. Approach of $(SiOHClH)_2O$ to $Si_{32}O_{48}H_{32}$ for reaction pathway (step 2).

mol was found for TS_1, and the system is stabilized to 16.0 kcal/mol for I_1 relative to the separate reactants. In the next step TS_2, the $Si_5–O_{35}$ bond of the cage is further loosened with a relative energy of only 16.5 kcal/mol before the system can stabilize itself in I_2 to 3.3 kcal/mol by rearrangement after complete breaking of the $Si_5–O_{35}$ bond. In the next transition structure TS_3, the newly formed $O_{35}–H_{113}$ bond links to the $Si_{107}–Cl_{114}$ bond of the remaining reagent. In I_3, the $Si_{107}–O_{35}$ bond is formed under elimination of HCl and the relative energy is lowered to −14.3 kcal/mol. Now the other $O_{110}–H_{115}$ group of the reagant reacts with the $Si_3–O_{32}$ bond between the heptagon and the hexagon of the cage. The relative energy is going up to 30.6 kcal/mol in TS_4. In I_4, the H_{115} atom binds to the O_{32} atom with a stabilization to 30.6 kcal/mol. The next transition structure TS_5 is characterized by a stronger $Si_3–O_{110}$ bonding and a substantial weakening of the $Si_3–O_{32}$ bond. The relative energy is now 14.5 kcal/mol. Rearrangement in I_5 leads to a stabilization of −8.9 kcal/mol. The final transition structure TS_6 with a relative energy value of 22.1 kcal/mol involves the interaction of the $O_{32}–H_{115}$ bond with the $Si_{109}–Cl_{116}$ bond, before HCl is eliminated and the last Si−O bond is formed in the product with a relative energy of −28.9 kcal/mol with respect to the reactants.

This reaction can start also at the two hexagons (Figure 5). We call this pathway b. A similar sequence of steps is involved and shown in Figure 6. The initial barrier is again 39.9 kcal/

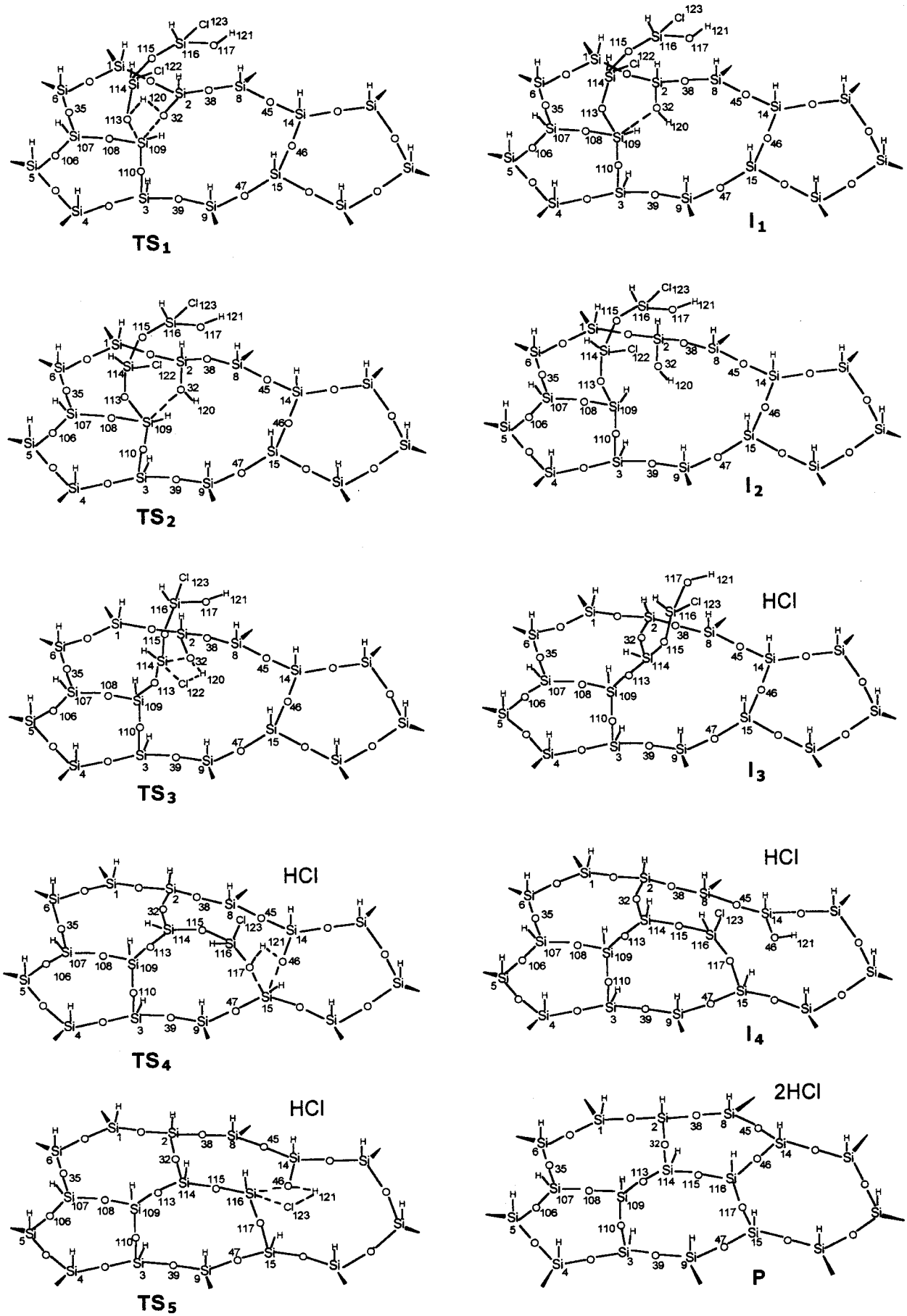

Figure 9. Transition structures TS and intermediates I for reaction pathway (step 2) from nonclassical structure $Si_{32}O_{48}H_{32}$ to classical structure $Si_{34}O_{51}H_{34}$.

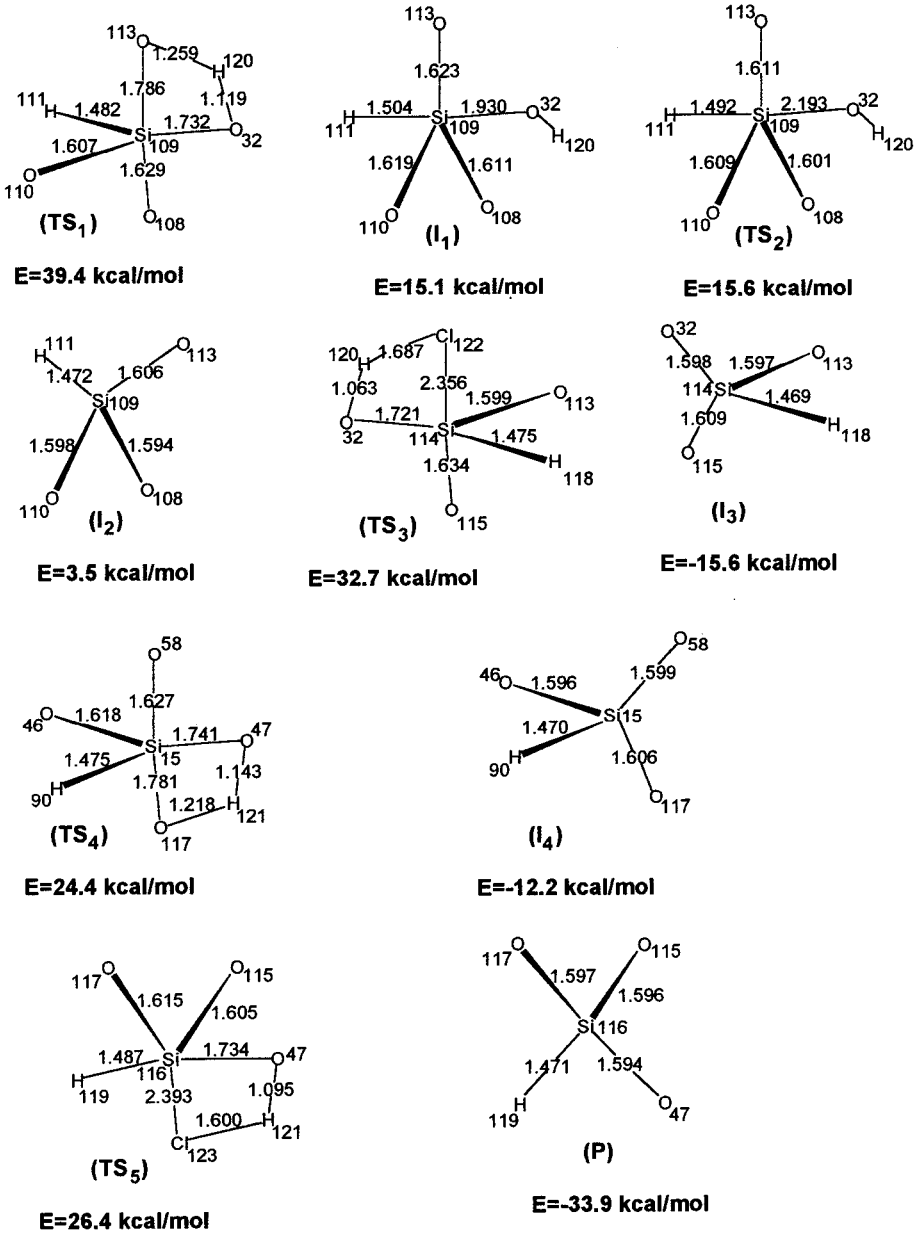

Figure 10. Energy and structure data for reaction pathway (step 2).

mol. It is again the highest (Figure 7). The sequence of energies is very similar to the one of pathway a, except that we did not find the equivalent of transition structure TS_5 of pathway a in the alternative pathway b. However, the barrier from I_4 to TS_5 was less than 1 kcal/mol and therefore insignificant. The final product is the same for both pathways and contains a heptagon. We call it therefore a nonclassical structure. The largest barrier of 39.9 kcal/mol is almost the same as the largest barrier of 40.1 kcal/mol for the classical pathway.[26]

3.2 Conversion of $Si_{32}O_{48}H_{32}$ to $Si_{34}O_{51}H_{34}$.

It is now essential to see whether the consecutive growth leading from the nonclassical structure of $Si_{32}O_{48}H_{32}$ to a classical structure of $Si_{34}O_{51}H_{34}$ is equally feasible.

We therefore studied the step 2 reaction in the same way, calculating transition structures TS and intermediates I. Figure 8 shows the initial arrangement in the region of interest. In Figure 9, the various transition structures and intermediates are presented. The idea was the same as in step 1. An OH group of the reagent $(SiOHClH)_2O$ approaches an SiO bond of the $Si_{32}O_{48}H_{32}$ cage. It involves a barrier of 39.4 kcal/mol for TS_1 (Figure 10). The Si−O bond of the cage is broken and a new Si−O bond between the cage and the reagent is formed. At the same time, an O−H bond is formed between cage and reagent. The system is stabilized to 15.1 kcal/mol in I_1. The next sequence of steps is very similar to those already encountered in pathway b of step 1. The energies vary from those of step 1 only by a few kcal/mol. Again the first barrier is the largest.

4. Conclusion

In a representative study of the growth of silsesquioxanes via an insertion mechanism, we have shown that reaction pathways which involve nonclassical structures of cages with heptagons are equally feasible as classical pathways involving cages with hexagons and pentagons only. The first barrier is the highest in all cases. The highest activation energy for the classical pathway with a value of 40.1 kcal/mol for the formal insertion of $Si_2O_3H_2$ to $Si_{30}O_{45}H_{30}$ is practically the same as the 39.9 kcal/mol barrier leading to a nonclassical structure of $Si_{32}O_{48}H_{32}$. The subsequent step back to a classical structure of $Si_{34}O_{51}H_{34}$ has a barrier (39.4 kcal/mol) in the same range. We

therefore expect that such nonclassical structures are involved in the formation of large silsesquioxanes.

Acknowledgment. This research was partially supported by Deutsche Forschungsgemeinschaft.

References and Notes

(1) Binnewies, M.; Jerzembek, M.; Kornik, A. *Angew. Chem.* **1991**, *103*, 762.
(2) Binnewies, M.; Jug, K. *Eur. J. Inorg. Chem.* **2000**, 1127.
(3) Quellhorst, H.; Wilkening, A.; Binnewies, M. *Z. Allg. Anorg. Chem.* **1997**, *623*, 1871.
(4) Binnewies, M.; Jerzembek, M.; Wilkening, A. *Z. Allg. Anorg. Chem.* **1997**, *623*, 1875.
(5) Wilkening, A. Ph.D. Thesis, Universität Hannover, 1998.
(6) Jutzi, P.; Batz, C.; Mutluay, A. *Z. Naturforsch.* **1994**, *49b*, 1689.
(7) Calzaferri, G. In *Taylor-made Silicon−Oxygen Compounds*; Corriu, R., Jutzi, P., Eds.; Vieweg: Wiesbaden, Germany, 1996; p 149.
(8) Bassindale, A. R.; Gentle, T. E.; Taylor, P. G.; Watt, A. In *Taylor-made Silicon−Oxygen Compounds*; Corriu, R., Jutzi, P., Eds.; Vieweg: Wiesbaden, Germany, 1996; p 171.
(9) Kuznetzov, V. L.; Usoltseva, A. N. In *Taylor-made Silicon−Oxygen Compounds*; Corriu, R., Jutzi, P., Eds.; Vieweg: Wiesbaden, Germany, 1996; p 193.
(10) Agaskar, P. A.; Klemperer, W. G. *Inorg. Chim. Acta* **1995**, *299*, 355.
(11) Agaskar, P. A.; Day, V. W.; Klemperer, W. G. *J. Am. Chem. Soc.* **1987**, *109*, 5554.
(12) Rikowski, E.; Marsmann, H. C. *Polyhedron* **1997**, *16*, 3357.
(13) Krüger, R. P.; Much, H.; Schulz, G.; Rikowski, E. *Monatsh. Chem.* **1999**, *130*, 163.
(14) Jug, K.; Wichmann, D. *J. Mol. Struct. (Theochem)* **1997**, *398−399*, 365.
(15) Wichmann, D.; Jug, K. *J. Phys. Chem. B* **1999**, *103*, 10087.
(16) Ahlswede, B.; Jug, K. *J. Comput. Chem.* **1999**, *20*, 563.
(17) Ahlswede, B.; Jug, K. *J. Comput. Chem.* **1999**, *20*, 572.
(18) Nanda, D. N.; Jug, K. *Theor. Chim. Acta* **1980**, *57*, 95, 107, 131.
(19) Jug, K.; Iffert, R.; Schulz, J. *Int. J. Quantum Chem.* **1987**, *32*, 265.
(20) Jug, K.; Iffert, R. *J. Comput. Chem.* **1988**, *9*, 51.
(21) Jug, K.; Krack, M. *Int. J. Quantum Chem.* **1992**, *44*, 517.
(22) Fowler, P. W.; Manolopoulos, D. E. *An Atlas of Fulerenes*; Clarendon Press: Oxford, U.K., 1995.
(23) Jug, K.; Wichmann, D. *J. Comput. Chem.* **2000**, *21*, 1549.
(24) Seifert, G.; Köhler, T.; Urbassek, H. M.; Hernandez, E.; Frauenheim, T. *Phys. Rev. B* **2001**, *63*, 193409.
(25) Seifert, G.; Frauenheim, T.; Köhler, T.; Urbassek, H. M. *Phys. Status Solidi B* **2001**, *225*, 393.
(26) Jug, K.; Gloriozov, I. P. *Phys. Chem. Chem. Phys.* in press.
(27) Ayuela, A.; Fowler, P. W.; Mitchell, D.; Schmidt, R.; Seifert, G.; Zerbetto, F. *J. Phys. Chem.* **1996**, *100*, 15634.
(28) Pyo, S.; Shu, L. H.; Echegoyen, L. *Tetrahedron Lett.* **1998**, *39*, 7653.
(29) Sen, R.; Sumathy, R.; Satishkumar, B. C. *J. Mol. Struct.* **1997**, *437*, 11.
(30) Saito, R.; Dresselhaus, G.; Dresselhaus, M. S. *Chem. Phys. Lett.* **1992**, *195*, 537.
(31) Fowler, P. W.; Heine, T.; Mitchell, D.; Orlandi, G.; Schmidt, R.; Seifert, G.; Zerbetto, F. *J. Chem. Soc., Faraday Trans.* **1996**, *92*, 2203.
(32) Xiang, K.-H.; Pandey, R.; Pernisz, U. C.; Freeman, C. *J. Phys. Chem. B* **1998**, *102*, 8704.
(33) Cheng, W.-D.; Xiang, K.-H.; Pandey, R.; Pernisz, U. C. *J. Phys. Chem. B* **2000**, *104*, 6737.